PHYSICAL REVIEW E VOLUME 56, NUMBER 4 OCTOBER 1997

Spatiotemporal solitons in multidimensional optical media with a quadratic nonlinearity

Boris A. Malomed*
Department of Interdisciplinary Studies, Faculty of Engineering, Tel Aviv University, Tel Aviv 69978, Israel

P. Drummond and H. He
Department of Physics, University of Queensland, St. Lucia, Queensland 4067, Australia

A. Berntson, D. Anderson, and M. Lisak
Institute for Electromagnetic Field Theory, Chalmers University of Technology, Gothenburg, S-41296, Sweden

(Received 24 March 1997)

We consider solutions to the second-harmonic generation equations in two- and three-dimensional dispersive media in the form of solitons localized in space and time. As is known, collapse does not take place in these models, which is why the solitons may be stable. The general solution is obtained in an approximate analytical form by means of a variational approach, which also allows the stability of the solutions to be predicted. Then, we directly simulate the two-dimensional case, taking the initial configuration as suggested by the variational approximation. We thus demonstrate that spatiotemporal solitons indeed exist and are stable. Furthermore, they are not, in the general case, equivalent to the previously known cylindrical spatial solitons. Direct simulations generate solitons with some internal oscillations. However, these oscillations neither grow nor do they exhibit any significant radiative damping. Numerical solutions of the stationary version of the equations produce the same solitons in their unperturbed form, i.e., without internal oscillations. Strictly stable solitons exist only if the system has anomalous dispersion at both the fundamental harmonic and second harmonic (SH), including the case of zero dispersion at SH. Quasistationary solitons, decaying extremely slowly into radiation, are found in the presence of weak normal dispersion at the second-harmonic frequency. [S1063-651X(97)14009-0]

PACS number(s): 42.65.Tg, 42.65.Ky

I. INTRODUCTION

The concept of optical spatiotemporal solitons (STS) [1] (frequently called ''light bullets'') has been attracting a lot of attention as a unique opportunity to create a self-supporting fully localized object freely propagating in a nonlinear medium. However, it is well known that STS in media with a Kerr (cubic) nonlinearity are strongly unstable, being subject to wave collapse [2]. The collapse can be prevented if one takes into account saturation of the nonlinearity [3]. Another more promising way is to use a medium with a quadratic nonlinearity. The absence of wave collapse in two- and three-dimensional [(2+1)D and (3+1)D] second-harmonic-generating (SHG) media has been demonstrated analytically [4] and numerically [5] (see also [6] and [7]). Moreover, in Ref. [4] it was proven, by means of rigorous variational estimates, that in both cases the model must have stable fully localized solitary-wave solutions realizing a nontrivial minimum of the Hamiltonian. In most of these calculations, a type of rotational symmetry between the space and time coordinate was assumed that is not found in practice. The treatment of more general nonsymmetric cases is the objective of the present work.

SHG media are now the focus of attention as a new field of nonlinear optics, especially as concerns solitons [8–15]. Thus far, temporal solitons have not been experimentally observed in quadratically nonlinear media. However, time-independent spatial solitons have been successfully generated in 2D (planar waveguide) [9] and 3D (bulk) [10] geometries. In this work, we will demonstrate that, by adding temporal dispersion to the spatial diffraction, one can construct stable STS in both geometries. Including the temporal variable, we will refer to these two cases as (2+1)D and (3+1)D geometries. The transverse dimension (equal to 2 and 3 in the former and latter cases, respectively) will be denoted d. As demonstrated in [4], wave collapse in the SHG system does not take place if the transverse dimension d, including the transverse coordinates and time, is smaller than 4. Thus, a self-focusing collapse is precluded in any physical dimension.

A. Parametric wave equation

The scaled equations describing copropagation of the fundamental harmonic (FH) and second harmonic (SH) in the quadratic medium have already been formulated in ([4]):

$$iu_\xi+\nabla_\rho^2 u+u_{\tau\tau}-u+vu^*=0, \tag{1}$$

$$2iv_\xi+\nabla_\rho^2 v+\delta v_{\tau\tau}-\gamma v+\frac{1}{2}u^2=0, \tag{2}$$

where $u=\sqrt{2}z_0\omega_1^2\mathcal{E}_1 e^{-iz/z_0}\chi^{(2)}/(k_1c^2)$ and $v=z_0\omega_1^2\mathcal{E}_2 e^{-2iz/z_0}\chi^{(2)}/(k_1c^2)$ are the scaled FH and SH envelopes, $\mathcal{E}_j$ are electric field envelope functions at frequency $j\omega_1$, $\xi=z/z_0$ and $\tau=(t-z/v_g)/t_0$ [14] are the scaled propagation distance and the scaled local time coordinate, at a group velocity v_g.

*Electronic address: malomed@eng.tau.ac.il

Here t_0 is a characteristic time scale used for scaling purpose, while $z_0=2t_0^2/k_1''$. The dimensionless transverse spatial coordinate ρ is defined by $\rho=\sqrt{x^2+y^2}/r_0$, where $r_0^2=(z_0/2k_1)$, given a carrier wave number of $k_1=k(\omega_1)$ at the (FH) frequency ω_1. The second order nonlinear Bloembergen coefficient is $\chi^{(2)}$, and the envelope function $\mathcal{E}_j$ is defined so that

$$E(t,\vec{x})=\sum_{j=1,2}\mathcal{E}_j(t,\vec{x})e^{-ij(\omega_1 t-k_1 z)}+\text{c.c.}. \tag{3}$$

The $(d-1)$-dimensional Laplacian $\nabla_\rho^2=\partial^2/\partial\rho^2+[(d-1)/\rho]\partial/\partial\rho$ acts upon the transverse spatial coordinate(s) [in the (3+1)D case, we will assume cylindrical symmetry], and the positive parameter γ measures the phase mismatch between the two harmonics, so that $\gamma=4+2z_0[2k(\omega_1)-k(2\omega_1)]$. The dispersion at the FH is assumed to be anomalous, and $\delta=k_2''/k_1''$ is the ratio of the SH and FH dispersion coefficients, which may have any sign. Equations (1) and (2) implicitly assume equal group velocities at the chosen carrier wavelengths, and are defined relative to envelope functions of form e^{ikz} and e^{2ikz}, respectively, which carry the usual propagation constant. We note here that the use of a moving frame coordinate system means that the first-order derivative in the equation is in the spatial propagation direction, ξ, while the transverse dimensions have both a spatial and temporal nature.

In this work, we will demonstrate that [at least in the (2+1)D case] STS's exist, in the rigorous sense, only if the SH dispersion is anomalous, i.e., if $\delta>0$, including also the zero-dispersion case $\delta=0$. However, if the dispersion at SH is weakly normal, a ''quasisoliton'' solution is possible. It decays into radiation so slowly that it may be regarded as quasistable.

B. Outline

The rest of the paper is organized as follows. In Sec. II, we develop an explicit analytical approximation for the solutions, both for the (3+1)D and (2+1)D cases, based on variational methods. The stability of the analytical solutions is tested by means of the known integral (Vakhitov-Kolokolov) criterion. Using the variational Gaussian approximation as the initial condition we present, in Sec. III, results of direct simulations of Eqs. (1) and (2) for the (2+1)D case, which demonstrate that STS's exist and are stable. Direct simulations of the (3+1)D case, which are more difficult technically, are deferred to another paper. An important conclusion is also that, although the variational approximation is not very precise in the (2+1)D case, it still provides a reasonable initial guess for the simulations, and it is therefore quite useful.

In Sec. IV, we summarize the obtained results and also briefly discuss possibilities for implementation of optical STS in an experiment. We infer that this should be possible if the FH pump wave is launched at a wavelength $\sim 3\mu$m (in the near infrared region), or, alternatively, optical STS can be realized as a gap soliton.

II. VARIATIONAL APPROXIMATION

We are interested in stationary (z-independent) solutions to Eqs. (1) and (2), and in their stability. In the (3+1)D case, we assume an axial symmetry for the transverse coordinate. Thus, a stationary solution is assumed to be given by the following PDE's for the *real* functions u and v:

$$u_{\rho\rho}+(d-2)\rho^{-1}u_\rho+u_{\tau\tau}-u+vu=0, \tag{4}$$

$$v_{\rho\rho}+(d-2)\rho^{-1}v_\rho+\delta v_{\tau\tau}-\gamma v+\frac{1}{2}u^2=0, \tag{5}$$

where ρ is the so-called radial coordinate in the case $d=3$, or simply the single transverse coordinate x in the case $d=2$.

Exact solutions to Eqs. (3) and (4) are not available in either case. We will show that, nevertheless, solutions can be effectively approximated by means of the analytical variational approach. Recently, this approach was used to treat a related but simpler problem, viz., spatial solitons supported by a quadratic nonlinearity in the (1+1)D and (2+1)D (rotationally symmetric) geometries [11].

A. Gaussian ansatz

The variational approach is based on a certain *ansatz* for the solution sought for [16]. A general property of solitons in the SHG model is a difference in spatial and temporal widths of their two components. The only tractable ansatz compatible with this property is the Gaussian variational approximation [11], which we will abbreviate as GVA:

$$u=A\exp(-a\rho^2-\alpha\tau^2),\quad v=B\exp(-b\rho^2-\beta\tau^2). \tag{6}$$

Here the arbitrary parameters a,b, α,β, and A,B represent, respectively, the inverse squared spatial and temporal widths and amplitudes of the FH and SH components of the soliton. The next ingredient of the variational technique is the Lagrangian of Eqs. (4) and (5), $L=\int_{-\infty}^{+\infty}d\rho\int_{-\infty}^{+\infty}d\tau\mathcal{L}$ in the case $d=2$, and $L=\int_0^\infty\rho d\rho\int_{-\infty}^{+\infty}d\tau\mathcal{L}$ in the case $d=3$, with the Lagrangian density

$$\mathcal{L}=\frac{1}{2}[(\nabla_\rho u)^2+(\nabla_\rho v)^2+u_\tau^2+\delta v_\tau^2+u^2+\gamma v^2-u^2 v]. \tag{7}$$

Before proceeding further with the variational approach, it is relevant to mention that the underlying equations (1) and (2) have three integrals of motion. One of them is the (transverse) momentum, which is zero for the ansatz (6). The other integral is the norm (also frequently called energy) W with the density

$$\mathcal{W}=|u|^2+4|v|^2. \tag{8}$$

The norm is related to its density $\mathcal{W}$ the same way the Lagrangian is related to its density (7). This quantity is actually proportional to the conserved Manley-Rowe photon number invariant, N_1+2N_2. The last one is the Hamiltonian of the full wave equations (1) and (2). For the real z-independent

solutions, it coincides with the above Lagrangian. The norm will be used below to obtain some estimates of the stability of the STS.

Coming back to the variational approach, we insert the ansatz Eq. (6) into Eq. (7). Integrating the resultant expression over ρ and τ, it is straightforward to find the corresponding *effective* Lagrangian. Finally, the equations for the parameters of the ansatz can be obtained by equating the variation of the effective Lagrangian to zero.

1. Two transverse dimensions

For two transverse dimensions, one time and one space (i.e., $d=2$), the expressions for the amplitudes are

$$A^2=\frac{(2a+b)(a+\alpha+1)(b+\delta\beta+\gamma)(2\alpha+\beta)}{2\sqrt{ab\alpha\beta}}, \tag{9}$$

$$B=\frac{1}{2}(a+\alpha+1)\sqrt{\frac{(2a+b)(2\alpha+\beta)}{a\alpha}}, \tag{10}$$

and the SH widths are eliminated as follows:

$$\beta=4\alpha^2(a-\alpha+1)^{-1}, \tag{11}$$

$$b=4a^2(\alpha-a+1)^{-1}. \tag{12}$$

The remaining equations for the FH widths take the form

$$2b(b+\delta\beta+\gamma)=(2a+b)(-b+\delta\beta+\gamma), \tag{13}$$

$$2\beta(b+\delta\beta+\gamma)=(2\alpha+\beta)(b-\delta\beta+\gamma). \tag{14}$$

2. Three transverse dimensions

For three transverse dimensions, one time and two space (i.e., $d=3$), one can first of all eliminate the amplitudes,

$$A^2=\frac{(2a+b)^2(2a+\alpha+1)(2b+\delta\beta+\gamma)(2\alpha+\beta)}{4ab\sqrt{\alpha\beta}}, \tag{15}$$

$$B=\frac{(2a+b)(2a+\alpha+1)}{2a}\sqrt{\frac{2\alpha+\beta}{2\alpha}}, \tag{16}$$

and then the SH temporal and spatial widths,

$$\beta=4\alpha^2(2a-\alpha+1)^{-1}, \tag{17}$$

$$b=4a^2(\alpha+1)^{-1}. \tag{18}$$

The remaining equations for the FH widths are

$$2b(2b+\delta b+\gamma)=(2a+b)(\delta\beta+\gamma), \tag{19}$$

$$2\beta(2b+\delta b+\gamma)=(2\alpha+\beta)(2b-\delta\beta+\gamma), \tag{20}$$

where b and β should be substituted from Eqs. (17) and (18).

Notice that Eqs. (13) and (14) or (19) and (20) can easily be solved for the mismatch and dispersion parameters γ and δ if one regards the widths α and a as given free parameters.

B. Symmetric dispersion case

It is relevant to consider in more detail the symmetric case $\delta=1$, when the FH and SH dispersions are equal. In this case, Eqs. (1) and (2) demonstrate a formal isotropy, mixing the transverse coordinates and time. Introducing the variable $\sigma\equiv\sqrt{\rho^2+\tau^2}$, one can replace Eqs. (3) and (4) by the ODE's,

$$u''+d\sigma^{-1}u'-u+vu=0, \tag{21}$$

$$v''+d\sigma^{-1}v'-\gamma v+\frac{1}{2}u^2=0, \tag{22}$$

the prime standing for $d/d\sigma$. In the case $d=2$, Eqs. (21) and (22) coincide with those describing spatial (cylindrical) solitons in three dimensions. These equations were recently considered in detail in [12] and [11]. For the case $d=3$, Eqs. (22) and (21) were recently solved numerically in [14]. The GVA also simplifies in the case $\delta=1$. In this case, one obtains physical solutions only with $\alpha=a$ and $\beta=b$.

1. Two transverse dimensions

For two transverse dimensions (one space and one time), i.e., $d=2$ and $\delta=1$, the SH width can also be eliminated: $b=4a^2$. The equation for the FH width becomes

$$\gamma=\frac{32a^3}{1-2a}. \tag{23}$$

This implies the restriction $a<\frac{1}{2}$ (since γ is positive). Thus, in (2+1) dimensions the ''isotropic'' solitons cannot be too narrow, but can be arbitrarily broad.

In [11] it was shown in detail that the variational approximation based on GVA furnishes a reasonably accurate description of the spatial cylindrical soliton, if compared to the numerical results [although somewhat less good than in the (1+1) dimensions, in which GVA produces an extremely good accuracy, as was demonstrated in the same work]. Due to the equivalence of the cylindrical soliton to STS with $\delta=1$ in (2+1) dimensions, we can thus use the results of [11] to justify the use of GVA in this case. More precise comparison with exact numerical simulations will be given later.

2. Three transverse dimensions

For $d=3$, there are three transverse dimensions (two space and one time). The SH width can be eliminated, $b=4a^2/(a+1)$, and the FH width is then determined by the cubic equation

$$36a^3+(\gamma-4)a^2-\gamma=0. \tag{24}$$

Equation (24) can be readily shown to have exactly one physical root for any value of the (positive) mismatch γ. Moreover, solving Eq. (24) for γ yields

$$\gamma=2a^2(9a-1)/(1-a^2), \tag{25}$$

which has an important consequence: the ''isotropic'' FH width a may take only the values $\frac{1}{9}<a<1$. In other words, the variational approximation predicts that, in the case $\delta=1$, solitons in (3+1) dimensions can neither be very broad ($a>\frac{1}{9}$) nor very narrow ($a<1$).

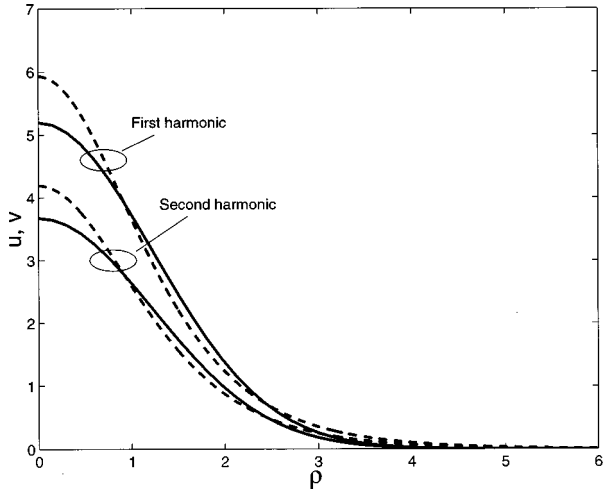

FIG. 1. Comparison of the variational (solid) and numerical (dashed) shapes of the initial $(3+1)$-dimensional spatiotemporal soliton in the ''isotropic'' case, $\delta=1$, for $\gamma=1$. The lower and upper curves show, respectively, the fundamental $u(\rho,\tau)$ and second harmonics, $v(\rho,\tau)$.

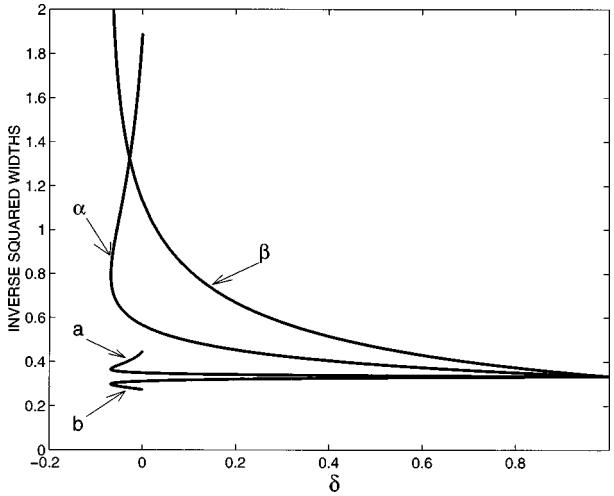

FIG. 2. The inverse squared widths of the spatiotemporal soliton [Eq. (6)] vs the relative dispersion parameter δ for $d=3$ and $\gamma=1$, as produced by the variational approximation.

For the case $\delta=1$, and $(3+1)$ dimensions (which corresponds to the case treated by Hayata and Koshiba [5]), we display in Fig. 1 the shape of the STS as predicted variationally, together with the numerically found shape taken from [14]. One concludes from Fig. 1, that GVA is less accurate in higher dimensions, but that it still gives a correct idea of the shape of the soliton. We emphasize again that this symmetric case of $\delta=1$ requires a matching of dispersion properties which is unlikely to occur in practice.

C. Existence range of variational solutions

Physical solutions are those for which all the widths a,b and α,β are real and positive. It follows from Eqs. (9) and (15) that positiveness of A^2 does not impose any additional constraint on selection of the solutions (at least, if $\delta>0$). Two interesting issues to be addressed are the existence range of the physical solutions, especially at zero and negative δ, and the possibility of multistability, i.e., having more than one physical solution for fixed γ and δ. Solving numerically the algebraic equations (13),(14) and (19),(20) for the FH widths, we arrive at the following conclusions: (i) At all positive γ and δ, there is exactly one physical solution (for both dimensions); (ii) for $d=2$, there is exactly one solution for *negative* δ too; (iii) for $d=3$, solutions for negative δ were found only in a very narrow stripe, e.g., at $\delta>-0.067$ for $\gamma=1$; (iv) in this narrow stripe (for $d=3$ only), the variational approximation produces *two* different solutions. The last two features are illustrated by Fig. 2, where we display the widths of the $(3+1)$D soliton vs the relative dispersion δ, as obtained from the GVA. We stress that these features need to be verified by full numerical simulations.

D. Stability

Later in this work, the variational approach will be compared with direct numerical simulations for $d=2$. It will be shown that the shape of the numerically found solitons is quite close to that obtained from the ansatz, provided that $\delta\geqslant 0$. The simulations will also demonstrate that, at negative δ, the solitons decay. This is not predicted by the GVA and is due to the fact that, as suggested by linearizing equation (2), the decay of the soliton at $\delta<0$ is accounted for by its ''tails.'' Obviously, GVA does not adequately approximate the exponentially decaying tails. Nevertheless, it will also be demonstrated that if δ is negative and small, the decay rate of the soliton predicted by GVA is so slow that it should be regarded as a quasistable (and therefore physically meaningful) state. This ''quasistability'' is enhanced if the mismatch parameter γ is large enough.

Some conclusions about the stability of the solitons can also be obtained within the framework of the GVA, using the known Vakhitov-Kolokolov (VK) stability criterion for solitons of the nonlinear Schrödinger type [17] (see also [2]). According to this criterion [which was recently applied to $(1+1)$D solitons in quadratically nonlinear medium [13] and to stationary cylindrical beams in [12]], a necessary condition for the stability of the soliton is a positive slope in the graph the soliton norm vs the propagation constant. Our solution does not explicitly contain the latter parameter.

In order to apply the VK criterion to Eqs. (1) and (2), one needs to perform a renormalization that expunges the mismatch γ from the equations, transforming it into an internal parameter of the solution family [12,13]. This transformation generates the above-mentioned propagation constant. In other words, we need to define a transformation of the form $(u,v,\gamma)\rightarrow(\widetilde{u},\widetilde{v},\widetilde{\gamma})$ such that if u,v are stationary solutions of the original equation with phase-match γ, then $\widetilde{u},\widetilde{v}$ are solutions to the equation with phase-match $\widetilde{\gamma}$. In this way, all solutions obtained by varying γ can be mapped into solutions of the same equation, but with different propagation constants—as required in the application of the VK criterion. The transformation can be written as

$$\widetilde{u}(\rho,\tau,\xi)=a^2u\left(\frac{\rho}{a},\frac{\tau}{a},\frac{\xi}{a^2}\right)e^{i\xi/a^2}, \tag{26}$$

$$\tilde{v}(\rho,\tau,\xi)=a^2 v\left(\frac{\rho}{a},\frac{\tau}{a},\frac{\xi}{a^2}\right)e^{i(2/a^2\pm 1)\xi}, \tag{27}$$

where $a=\sqrt{2/|4-\gamma|}$. In Eq. (27) ''+'' and ''−'' correspond to $\gamma<4$ and $\gamma>4$, respectively.

We choose $\tilde{\gamma}=2$ as the reference value for this purpose, leading to a ''renormalized norm'' $\tilde{W}$. After some manipulations, the renormalized norm $\tilde{W}$ takes the form

$$\tilde{W}=a^{(3-d)/2}W, \tag{28}$$

where W is defined by the density (8). It can also be shown that the necessary condition for stability of the soliton finally amounts to

$$\mathrm{sgn}(4-\gamma)\frac{d\tilde{W}}{d\gamma}>0. \tag{29}$$

[In the critical case of exact phase matching, $\gamma=4$, the transformation Eqs. (26) and (27) is singular and the criterion does not give a definite verdict.]

The dependences of the renormalized norm (28) vs γ for both cases $d=3$ and $d=2$, obtained from the GVA solution, are shown in Figs. 3(a) and 3(b) for two different values of the relative dispersion, $\delta=1$ and $\delta=0$. In the same figures, we show the values of the renormalized norm obtained from the full numerical solution in the special case $\delta=1$. Notice that Fig. 3 not only tells us about stability of the solitons, but also helps to estimate the accuracy of the GVA.

We conclude from Fig. 3 that, for each d and δ, there is a single critical value γ_{cr} of γ that separates, according to the criterion (29), stable solitons at $\gamma>\gamma_{\mathrm{cr}}$ and unstable ones at $\gamma<\gamma_{\mathrm{cr}}$. In the GVA approximation, these critical values at $d=3$ are $\gamma_{\mathrm{cr}}\approx 0.65$ for both $\delta=2$ and $\delta=0$. At $d=2$ they are $\gamma_{\mathrm{cr}}\approx 0.37$ for $\delta=2$ and $\gamma_{\mathrm{cr}}\approx 0.52$ for $\delta=0$. However, in the next section we will show numerical results that indicate that these predictions are unreliable for $\delta\leqslant 0$, where it seems that $\gamma_{\mathrm{cr}}\to\infty$.

The GVA predictions for the existence of the *stable* solitons in the cases $d=2$ and $d=3$ are summarized in Fig. 4, where we show a boundary curve separating stable and unstable solitons in the parametric plane (δ,γ). This plot is quite important by itself, and also because its portion (a) (pertaining to $d=2$) will be used in the next section for comparison with results of direct numerical simulations of the same case.

E. GVA accuracy

Our general inference, based on a comparison of Fig. 1(a) with similar figures from [11], is that the accuracy of GVA deteriorates with increasing dimensionality. We assume that this feature of GVA may be quite generic. The reason for this is that the soliton presumably has tails which decay at least exponentially at large radius, and the contribution of these tails is of increasing significance at larger dimensionality. These tails are suppressed by GVA, which has a more rapid (than exponential) cutoff at large radius.

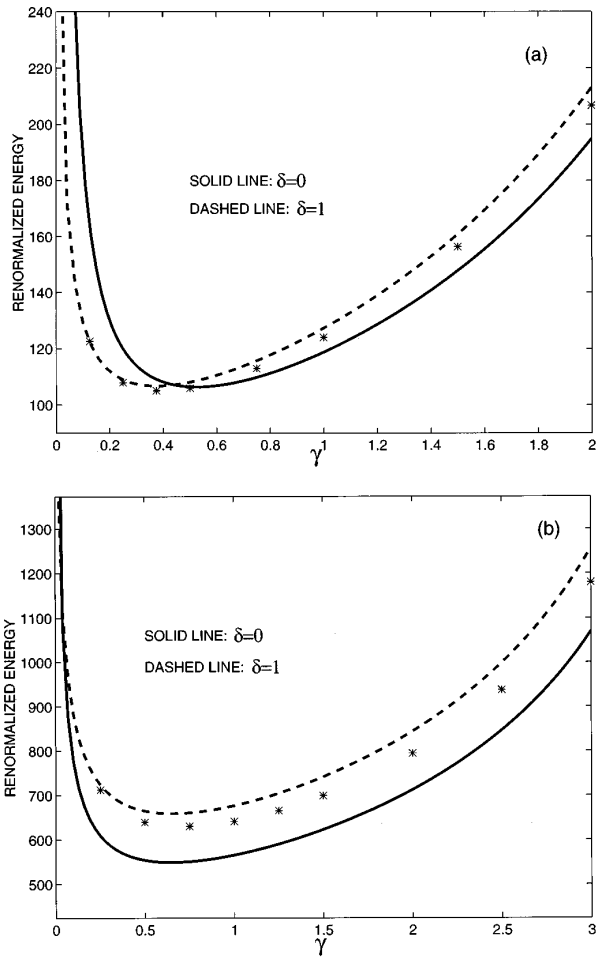

FIG. 3. The renormalized norm $\tilde{W}$ [Eq. (28)] vs the mismatch γ for the spatiotemporal soliton: (a) $d=2$; (b) $d=3$. The solid and dashed curves are obtained from the variational approximation for, respectively, $\delta=0$ and $\delta=1$. The stars are exact numerical results for $\delta=1$.

III. NUMERICAL RESULTS

Direct simulations of Eqs. (1) and (2) were performed for (2+1) dimensions, starting from an initial configuration suggested by the variational ansatz (6), with the parameters determined by Eqs. (11)–(14). When designing the Fourier-transform scheme for the numerical simulations [18], special care was taken to absorb periodic reflection of the emitted radiation from the edges of the integration domain, in order to avoid the so-called aliasing problem, when dynamics of the solitary wave can be distorted by its interaction with the reflected ''radiation.'' In all cases, discretization errors (due to finite step-size) were monitored and kept to a level of 1% or less. Typical lattice sizes employed were around 20 000 $\times 128\times 128$ points for the (2+1)D simulations.

For real physical applications, it is important to consider the case of small positive and general negative δ, as it is natural to expect that the dispersion at SH should be either essentially less anomalous than at FH, or normal.

A. Stable propagation: $\delta\geqslant 0$

In Fig. 5, we show a typical example of the evolution of the solitary wave generated by the variational ansatz at small

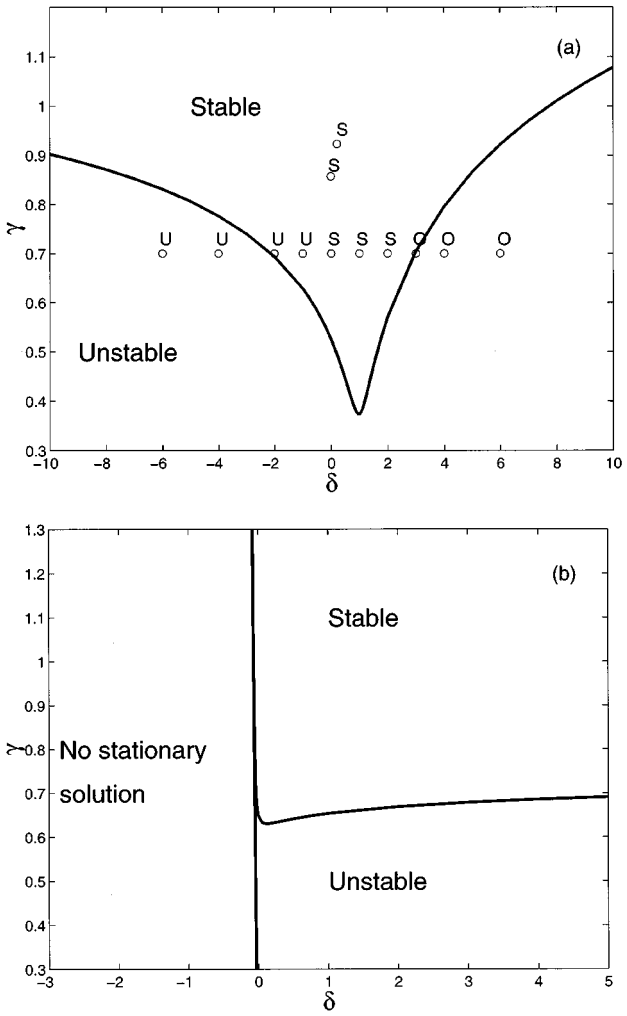

FIG. 4. The stability boundary for (a) (2+1)-dimensional and (b) (3+1)-dimensional spatiotemporal solitons on the parametric plane (δ,γ). In the portion (a), the circles correspond to the cases for which direct simulations have been run (see Figs. 5–7, 9, and 11 below). The marks *S*, *U*, and *O* are to distinguish between the cases in which the direct simulations have revealed, respectively, stability, instability (decay), and an oscillatory behavior of the soliton.

δ and relatively large phase mismatch parameter γ ($\delta=0.1430$, $\gamma=8.2868$). The variationally predicted ansatz generates a stable spatiotemporal solitary wave with some internal oscillations. A noticeable feature of the oscillations is that, while they are not growing and hence do not give rise to an instability, neither do they demonstrate any conspicuous radiative damping.

The stability of the soliton against internal vibrations and, simultaneously, the stability of the vibrations against radiative damping, even when the vibration amplitude is quite large, are known features of the usual (low-dimensional) SHG model [15]. Detailed analysis has demonstrated that these features are strongly related to the structure of internal modes of the dynamical soliton in this model: it has one genuine internal mode, and one ''quasimode'' belonging to the continuum spectrum. It was shown that the eigenfrequencies of the two modes are quite close (which gives rise to long-lived internal beatings of the perturbed soliton), and that even the quasimode, though it directly resonates with the

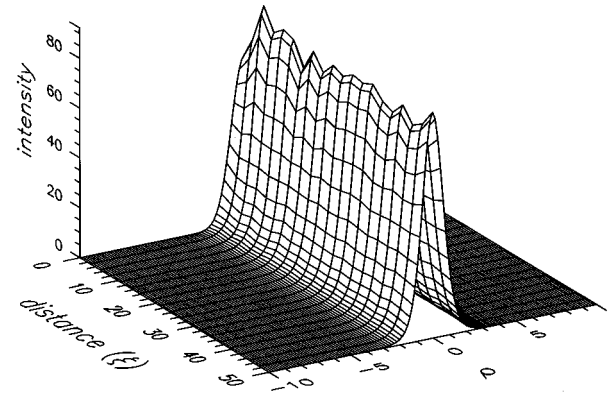

FIG. 5. An example of evolution of the spatiotemporal soliton in (2+1) dimensions, with a weak anomalous dispersion at the second harmonic, $\delta=0.1430$, and relatively large mismatch, $\gamma=8.2878$. The initial configuration is taken as per the variational ansatz (6). Shown is the cross section $\tau=0$ of the evolution of the fundamental intensity, i.e., $u^2(\rho,0,\xi)$.

radiation, decays extremely slowly. The study of internal modes of the multidimensional soliton is a challenging but much more complicated problem.

The smallness of δ does not essentially affect the accuracy of the variational approximation, as estimated by the amplitude of the internal oscillations of the soliton generated by the variationally predicted initial configuration, in comparison with the ''isotropic'' case $\delta=1$, which is displayed in Fig. 6. Another relevant example, pertaining to a smaller γ, is displayed in Fig. 7.

To check another general inference formulated in the preceding section, i.e., that the accuracy provided by the variational approximation deteriorates with increasing dimensionality, we have additionally run direct simulations of Eqs. (1) and (2) for the (1+1)-dimensional case, starting again from the variationally predicted ansatz. A typical example is shown in Fig. 8. One sees that, while the variational ansatz still produces some error, the error is conspicuously smaller than in the (2+1)-dimensional model, giving rise to internal oscillations with a smaller amplitude.

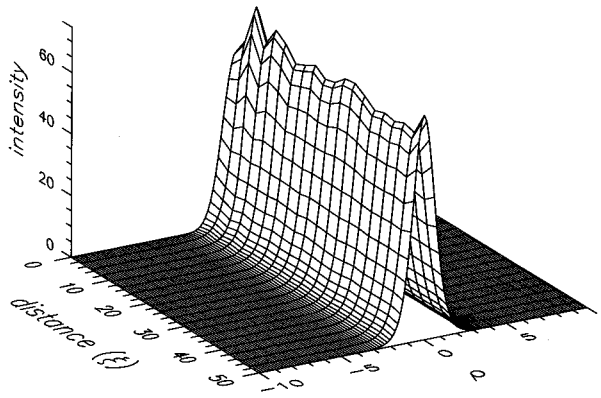

FIG. 6. Propagation of fundamental intensity $u^2(\rho,0,\xi)$ with an initial variational ansatz, for the ''isotropic'' case $d=2$, $\delta=1$, at $\gamma=6.75$.

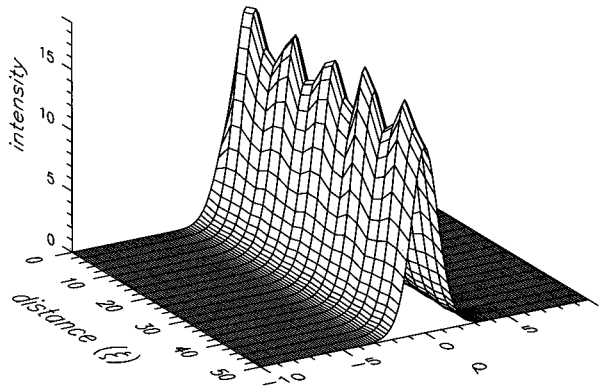

FIG. 7. Propagation of fundamental intensity $u^2(\rho,0,\xi)$ with an initial variational ansatz, for the case $d=2$, $\delta=0.2055$, and $\gamma=0.9229$.

B. Unstable propagation: $\delta \leqslant 0$

An issue of principal interest (first of all, for application to real physical media) is to check the possibility of the existence of solitons at $\delta<0$, when the SH dispersion is normal. As mentioned in the preceding section, the variational approximation [for the (2+1)-dimensional case] produces a solution at all negative δ, and the usual stability criteria indicate that these should be stable at large γ.

If $|\delta|$ is small, the pulse generated by GVA seems *practically stable*: its decay is so slow that it appears to be a fairly stable soliton that does not have any visible difference from the stable solitons found at positive δ. An example for $\delta=-0.01$ and $\gamma=0.8571$ is shown in Fig. 9. It is relevant to stress that at δ exactly equal to zero, when Eq. (2) does not contain the second time derivative, the soliton still exists and is very close to that shown in Fig. 9. We conjecture that the soliton exists in the rigorous sense if $\delta=0$. However, the simulations indicate that, strictly speaking, stable pulses do not exist at negative δ. This is especially true for large $|\delta|$, where the decay of the pulse is very rapid. An example is shown, for $\delta=-1$ and $\gamma=10$, in Fig. 10(a). At the same value of γ and moderately small $\delta=-0.1$, the soliton is quasistable [Fig. 10(b)]. As a general trend, we observed that

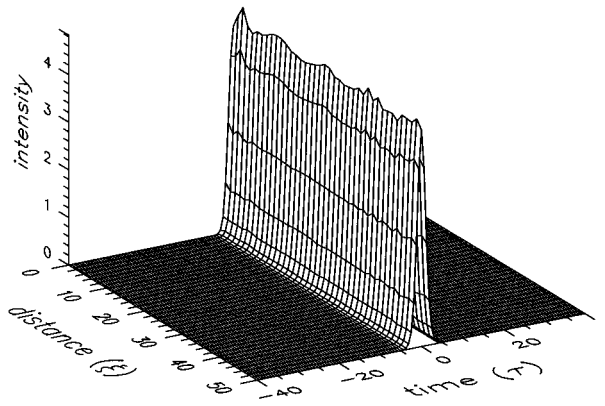

FIG. 8. An example of evolution of the pulse generated by the initial configuration taken as per the variational approximation in the (1+1)-dimensional case for $d=\delta=\gamma=1$. Displayed is the fundamental intensity $u^2(\tau,z)$.

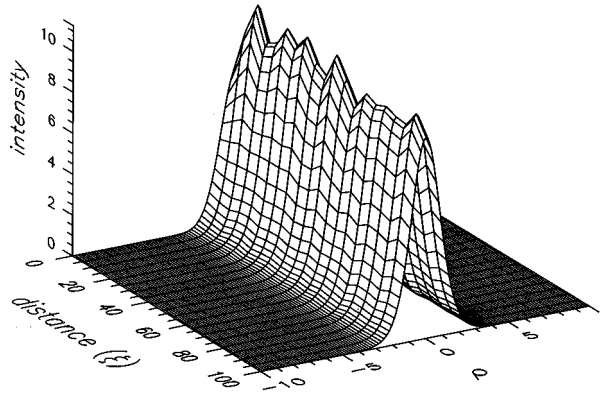

FIG. 9. Propagation of fundamental intensity $u^2(\rho,0,\xi)$ with an initial variational ansatz, for the case $d=2$, $\delta=-0.01$, and $\gamma=6/7$, showing quasistable propagation with normal dispersion at the fundamental wavelength.

a larger mismatch γ helped to effectively stabilize the pulses at negative δ.

All the cases considered above lay sufficiently deep inside the stability region predicted by GVA; see Fig. 4(a).

C. Stability boundary curve

We have performed another series of the simulations in order to check the stability boundary curve. To this end, a

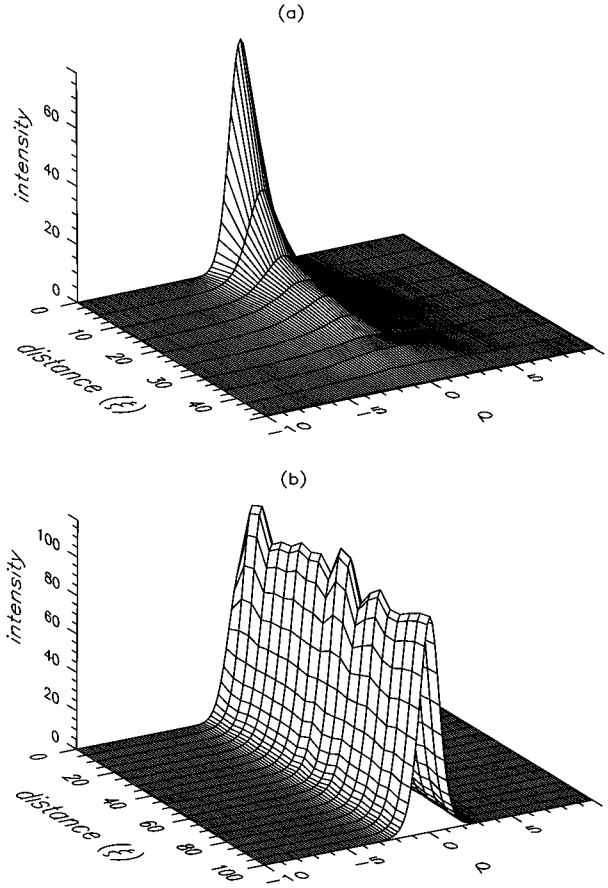

FIG. 10. Propagation of fundamental intensity $u^2(\rho,0,\xi)$ with an initial variational ansatz, for the cases $d=2$, $\gamma=10$ and (a) $\delta=-1.0$, (b) $\delta=-0.1$. This shows unstable and quasistable propagation, respectively.

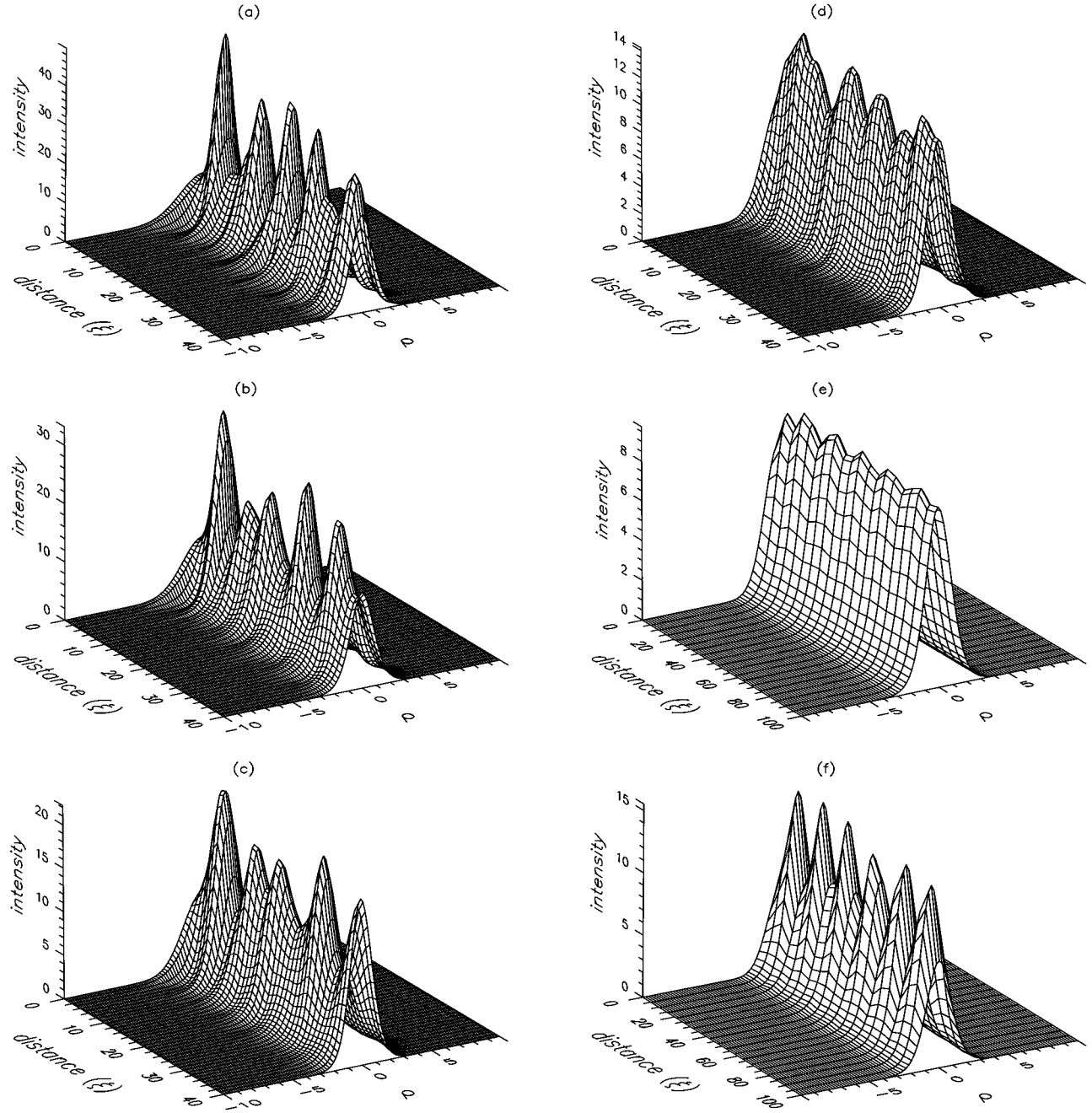

FIG. 11. Propagation of fundamental intensity $u^2(\rho,0,\xi)$ with an initial variational ansatz, for the cases $d=2$, $\gamma=0.7$ on the parametric plane of Fig. 4: (a) $\delta=+6$; (b) $\delta=+4$; (c) $\delta=+3$; (d) $\delta=+2$; (e) $\delta=+1$; (f) $\delta=0$; (g) $\delta=-1$; (h) $\delta=-2$; (i) $\delta=-4$; (j) $\delta=-6$.

string of parametric points along the line $\gamma=0.7$ (which is expected to intersect this stability boundary curve twice) was selected. The results are shown in Fig. 11. Comparing them with the location of the corresponding points in Fig. 4, one concludes that, provided $\delta\geqslant 0$, the points lying deep enough inside the regions that are expected to be stable indeed generate pulses that are stable [cases (d), (e), and (f)]. The points obtained for $\delta<0$ all decay rapidly [cases (g), (h), (i), and (j)], while cases outside the stability boundary in the region $\delta\gg 1$ show evidence of oscillatory behavior.

Thus, the stability boundary predicted by GVA proves to be rather ''fuzzy'' in comparison with the direct simulations, but, nonetheless, this border definitely has its meaning. However, one should notice, in accordance with what was said above, that the stability boundary predicted by GVA at negative δ appears to be incorrect, with the possible exception of cases where $|\delta|$ is very small.

Thus far, we have considered the evolution problem for a Gaussian initial pulse. The numerical solutions displayed above clearly demonstrate existence and stability of solitons both at positive and, effectively, at small negative δ and at arbitrary mismatch γ. However, they do not show the exact shape of the stationary soliton. This can be obtained from a numerical solution of the stationary version of Eqs. (1) and (2), i.e., the equations without the ξ derivatives. We do not pursue this problem here, since practical inputs in experiments are most likely to have a Gaussian-like shape. Exact solutions of the stationary problem are known when the soli-

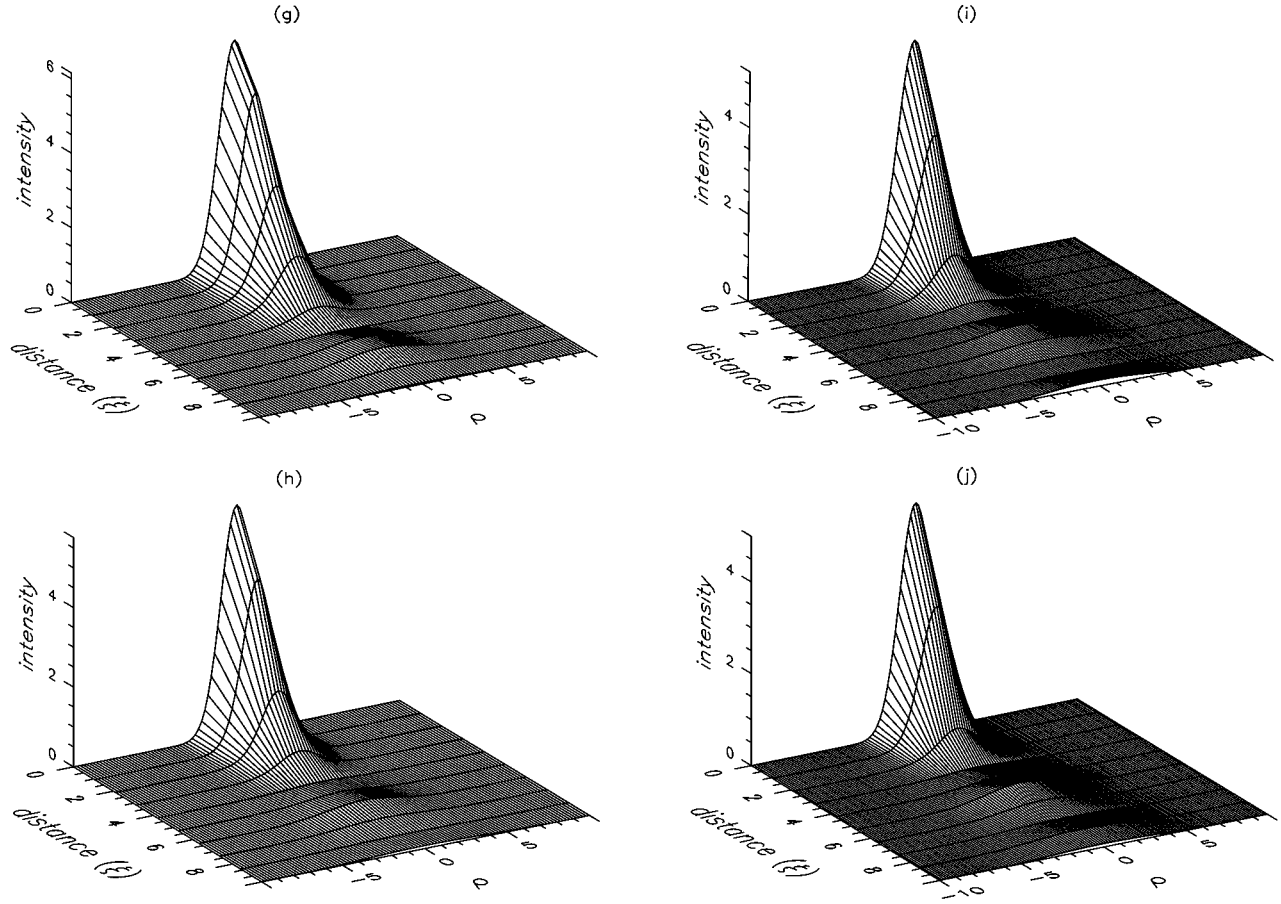

FIG. 11 (*Continued*).

ton is ''isotropic,'' i.e., in the physically unrealistic case $\delta=1$ (provided that the temporal and spatial variables have been appropriately rescaled). This rescaling to the formally isotropic form is not possible if $\delta\neq 1$.

We finally present here a snapshot of an ''asymmetric'' Gaussian initial pulse after propagating for a distance of 10. The parameters used here are $\delta=0$ and $\gamma=6/7$. Figures 12(a)–12(d) are the snapshots of both the first and the second harmonic from two different angles. Figures 12(e) and 12(f) are contour plots of the pulses. This result shows very strongly the anisotropic behavior caused by a small value of δ, which causes a distortion in the second-harmonic pulse shape.

IV. CONCLUSION

In this work, we have considered spatiotemporal solitary-wave solutions to the (2+1)D and (3+1)D second-harmonic-generation equations with group-velocity matching. Using the variational approach, we have constructed in an analytical form a full family of approximate soliton solutions for both cases. We have also tested their stability by means of the Vakhitov-Kolokolov criterion. Next, using the variational approximation as the initial condition, we have performed direct numerical simulations for (2+1) dimensions. We have found that the variationally predicted initial configurations give rise to stable solitary waves with some internal oscillations. The oscillations demonstrate almost no radiative damping. Stable solitons exist provided that the dispersion at both the fundamental and second harmonics is anomalous, including the case of zero dispersion at the second harmonic. If the second harmonic has a weak normal dispersion, an effectively stable quasisoliton is still possible.

As concerns the experimental search for multidimensional spatiotemporal solitons in higher dimensional second-harmonic-generating media, the fact that the dispersion at both harmonics should be anomalous is the most essential limitation. Typically this might require launching the fundamental harmonic with a wavelength $\geqslant 3\mu$m, if we assume anomalous dispersion is achieved for a second-harmonic wavelength above 1.5 μm. Next, it is necessary to match the group velocities of the harmonics. Another problem is the rather weak temporal dispersion of real media. Group velocity matching typically requires the use of birefringence, while weak dispersion implies rather long interaction lengths, unless the pulses are very short.

A powerful and elegant way to induce a strong *effective* dispersion in a medium with weak intrinsic dispersion is to use linearly coupled modes. The dispersion-generating coupling may be induced by the Bragg scattering in a medium with a resonant grating [19]. Another system in which essentially the same mechanism works is an asymmetric optical coupler (see, e.g., [20]). In either case, the soliton in such a system will be a so-called *gap soliton* [21,19].

Recently, gap solitons were analyzed in (1+1)-dimensional and (2+1)-dimensional second-harmonic-generating models [22]. The results showed that the gap soli-

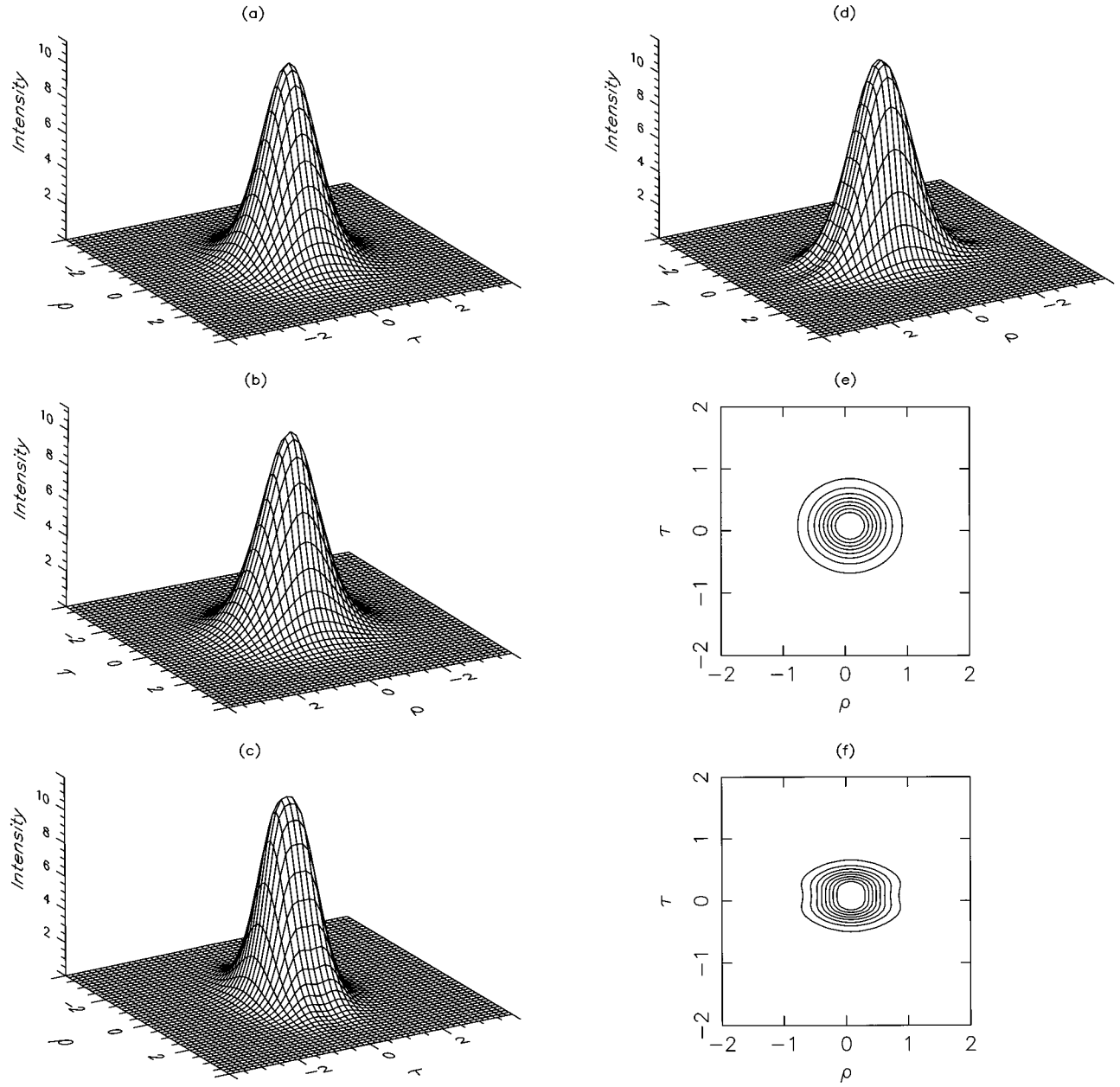

FIG. 12. Snapshots of an initial variational soliton at distance $\xi=10$ for $d=2$, $\delta=0$, $\gamma=6/7$. Displayed are views of the intensity profile $u^2(\rho,\tau,10)$ of the soliton's fundamental-harmonic component from two different directions, (a) and (b), second-harmonic component (c) and (d), and their level contours, i.e., a set of the cross sections by the (τ,ρ) plane (e) and (f).

ton equations can be mapped onto the present parametric equations, provided the effective mass approximation is valid (i.e., near the center of the band gap). In the multidimensional case, the necessary resonant grating can be implemented as a system of parallel scores on the planar waveguide, or as a layered structure in the bulk medium. As for the coupler, it does not exist in the $(3+1)$-dimensional case, but in $(2+1)$ dimensions it can be realized as a system of two parallel planar waveguides. This technique also reduces the difficulty of achieving the group-velocity matching. Analytical and numerical consideration of multidimensional gap solitons in the second-harmonic-generating media, as well as simulations of the usual soliton in the $(3+1)$ dimensions, are now underway [23].

In summary, it seems feasible that in at least one of these types of media, a well-defined stationary wave, localized in time and space, will be experimentally observed.

[1] Y. Silberberg, Opt. Lett. **15**, 1281 (1990).
[2] E. A. Kuznetsov, A. M. Rubenchik, and V. E. Zakharov, Phys. Rep. **142**, 105 (1986); J. J. Rasmussen and K. Rypdal, Phys. Scr. **33**, 481 (1986).
[3] D. E. Edmundson and R. H. Enns, Opt. Lett. **17**, 586 (1992).
[4] A. A. Kanashov and A. M. Rubenchik, Physica D **4**, 122 (1981).
[5] K. Hayata and M. Koshiba, Phys. Rev. Lett. **71**, 3275 (1993).
[6] L. Bergé, V. K. Mezentsev, J. J. Rasmussen, and J. Wyller, Phys. Rev. A **52**, R28 (1995).
[7] S. K. Turitsyn, Pis'ma Zh. Éksp. Teor. Fiz. **61**, 458 (1995) [JETP Lett. **61**, 469 (1995)].
[8] R. DeSalvo, D. Hagan, M. Sheik-Bahae, G. Stegeman, and E. Van Stryland, Opt. Lett. **17**, 28 (1992); G. I. Stegeman, M. Sheik-Bahae, E. Van Stryland, and G. Assanto, *ibid.* **18**, 13 (1993); R. Schiek, J. Opt. Soc. Am. B **10**, 1848 (1993); M. J. Werner and P. D. Drummond, *ibid.* **10**, 2390 (1993); A. V. Buryak and Y. S. Kivshar, Opt. Lett. **19**, 1612 (1994); Phys. Lett. A **197**, 407 (1995); L. Torner, C. M. Menyuk, and G. I. Stegeman, Opt. Lett. **19**, 1615 (1994); J. Opt. Soc. Am. B **12**, 889 (1995).
[9] W. E. Torruellas, Z. Wang, D. J. Hagan, E. W. Van Stryland, G. I. Stegeman, L. Torner, and C. R. Menyuk, Phys. Rev. Lett. **74**, 5036 (1995).
[10] R. Schiek, Y. Baek, and G. I. Stegeman, Phys. Rev. E **53**, 1138 (1996).
[11] V. Steblina, Y. S. Kivshar, M. Lisak, and B. A. Malomed, Opt. Commun. **118**, 345 (1995).
[12] A. V. Buryak, Yu. S. Kivshar, and V. V. Steblina, Phys. Rev. A **52**, 1670 (1995).
[13] D. E. Pelinovsky, A. V. Buryak, and Yu. S. Kivshar, Phys. Rev. Lett. **75**, 591 (1995).
[14] H. He, M. J. Werner, and P. D. Drummond, Phys. Rev. E **54**, 896 (1996).
[15] C. Etrich, T. Peschel, F. Lederer, B. A. Malomed, and Y. S. Kivshar, Phys. Rev. E **54**, 4321 (1996).
[16] D. Anderson, Phys. Rev. A **27**, 3135 (1983); D. Anderson, M. Lisak, and T. Reichel, J. Opt. Soc. Am. B**5**, 207 (1988).
[17] M. G. Vakhitov and A. A. Kolokolov, Radiophys. Quantum Electron. **16**, 783 (1973).
[18] P. D. Drummond, Comput. Phys. Commun. **29**, 211 (1983).
[19] U. Mohideen, R. F. Slusher, V. Mizrahi, T. Ergodan, M. Kuuwata-Gonokami, P. J. Lemaire, J. E. Sipe, C. Martijn de Sterke, and N. G. R. Broderick, Opt. Lett. **20**, 1674 (1995).
[20] B. A. Malomed, I. Skinner, P. L. Chu, and G. D. Peng, Phys. Rev. E **53**, 4084 (1996).
[21] A. B. Aceves and S. Wabnitz, Phys. Lett. **141**, 116 (1989).
[22] T. Peschel, U. Peschel, F. Lederer, and B.A. Malomed, in *Nonlinear Guided Waves and Their Applications*, OSA 1996 Technical Digest Series Vol. 15 (OSA, Washington, D.C., 1996), p. 52; and Phys. Rev. E **55**, 4730 (1997); H. He and P. Drummond, Phys. Rev. Lett. **78**, 4311 (1997).
[23] P. Drummond, H. He, and B.A. Malomed (unpublished).